Ocean Modelling 126 (2018) 77–84

Contents lists available at ScienceDirect

Ocean Modelling

journal homepage: www.elsevier.com/locate/ocemod

Short communication

Parameterizing unresolved obstacles with source terms in wave modeling: A real-world application

Lorenzo Mentaschi[a,*], Georgia Kakoulaki[b], Michalis Vousdoukas[a,c], Evangelos Voukouvalas[d], Luc Feyen[a], Giovanni Besio[e]

[a] European Commission, Joint Research Centre (JRC), Directorate for Space, Security and Migration, via Fermi 2749, 21027 Ispra VA, Italy
[b] Federal University of Pernambuco, Recife, Brazil.
[c] Department of Marine Sciences, University of the Aegean, University hill, 41100, Mitilene, Lesbos, Greece.
[d] Engineering Inegneria Informatica s.p.a, 56 via s. Martino della Battaglia 00185 Rome, Italy
[e] Università di Genova, Dipartimento di Ingegneria Chimica, Civile e Ambientale, via Montallegro 1, 16145 Genova, Italy

ARTICLE INFO

Keywords:
Wave modeling
Subscale modelling
Unresolved obstacles
Wavewatch
UOST
Source term

ABSTRACT

Parameterizing the dissipative effects of small, unresolved coastal features, is fundamental to improve the skills of wave models. The established technique to deal with this problem consists in reducing the amount of energy advected within the propagation scheme, and is currently available only for regular grids. To find a more general approach, Mentaschi et al., 2015b formulated a technique based on source terms, and validated it on synthetic case studies. This technique separates the parameterization of the unresolved features from the energy advection, and can therefore be applied to any numerical scheme and to any type of mesh. Here we developed an open-source library for the estimation of the transparency coefficients needed by this approach, from bathymetric data and for any type of mesh. The spectral wave model WAVEWATCH III was used to show that in a real-world domain, such as the Caribbean Sea, the proposed approach has skills comparable and sometimes better than the established propagation-based technique.

1. Introduction

Unresolved bathymetric and coastal features, such as cliffs, shoals and small islands, are a major source of local error in spectral wave models. Their dissipative effects can be accumulated over long distances and therefore, neglecting them, can compromise the simulation skills on large portions of the domain (Mentaschi et al., 2015a; Tolman, 2003; Tuomi et al., 2014). An established approach to subscale model these dissipative effect consists in attenuating the energy of the waves as they travel through partially obstructed cells, representing the unresolved features by means of transparency coefficients. This attenuation is typically implemented in the numerical scheme that models energy advection (Booij et al., 1999; Hardy et al., 2000; Tolman, 2014,2003). Generally, in this approach only 2 transparency coefficients are considered, for spectral components moving along the 2 axes of the mesh, though for some implementations the directional layout of the unresolved obstacles is considered (Hardy et al., 2000).

The introduction of this technique led to major improvements of the models' skill, but comes with an important drawback: the fact that it is implemented in the propagation scheme till now limited its application to the sole regular grids. This is due to a couple of reasons.

1) In principle, the established approach could be implemented in any numerical scheme based on cell boundary fluxes. However, some of the logics implemented in regular grids for subscale modelling are not immediately applicable to some of the other types of mesh. For example, in finite elements schemes the evolution of the spectral density is estimated in terms of flux convergence into the median dual cells associated with the nodes (Roland, 2008; Tolman, 2014; Zijlema, 2010). In such schemes, understanding the directionality of the reductions related with unresolved obstacles, and how these reductions should be combined, would not be straightforward.
2) Powerful, reliable and freely available tools exist for the automatic estimation of the unresolved obstacles in regular grids (e.g. Chawla and Tolman, 2008). For other types of mesh, like triangular meshes (Roland, 2008; Zijlema, 2010) or Spherical Multi-Cell (SMC) meshes (Li, 2011), these tools should be deeply revised.

These drawbacks impact both model developers (the cost of developing and testing the established technique might be high), and

* Corresponding author.
E-mail address: lorenzo.mentaschi@ec.europa.eu (L. Mentaschi).

https://doi.org/10.1016/j.ocemod.2018.04.003
Received 25 November 2017; Received in revised form 6 April 2018; Accepted 16 April 2018
Available online 17 April 2018

modelers (currently, a parameterization of unresolved obstacles, for meshes other than regular, does not exist).

We further need to say that the meshes of finite elements and SMC schemes are flexible, and in principle allow overcoming the problem of unresolved coastal features by increasing the grid resolution locally. However, this may result in computationally expensive meshes, especially for large scale models. Not to mention the overhead required to elaborate locally highly refined flexible meshes. Therefore, a good first-order parameterization of the effects of unresolved obstacles would be very useful also when using one of these schemes.

A possible solution to this problem is parameterizing the unresolved features with source terms, thus separating the parameterization of the unresolved obstacles from the energy propagation. The Unresolved Obstacles Source Term (UOST) was proposed by Mentaschi et al. (2015b) to this purpose, and models the effects of the subscale features on the cell where they are located, and their shadow on the downstream cells. UOST was tested in a set of ideal case studies, where its skills have been found to be close to the average skills of high resolution models (Mentaschi et al., 2015b).

In this manuscript, we present the first application of UOST to a real-world case (i.e., based on real-world bathymetry and wind data), that was possible only after the development of a software package (hereinafter referenced as alphaBetaLab) for the estimation of the transparency coefficients needed by the source term, from real bathymetric data. We focused our efforts on the Caribbean Sea, an area where the presence of many small islands and cliffs requires parameterization in low resolution models, due to their corresponding large impact on wave dynamics. We examined the performances of UOST on a time frame of 10 years (2000–2009), and compared it to the approach established in WW3 (Chawla and Tolman, 2008; Tolman, 2003).

In Section 2 a brief summary of UOST is given. Section 3 describes the simulations carried out in this study and the methodology used for validation and comparison. In Section 4, the model skill in the Caribbean sea is presented and discussed. Conclusions are finally drawn in Section 5.

2. Parameterizing unresolved features with source terms

The UOST/alphaBetaLab approach relies on the hypothesis that any mesh can be considered as a set of polygons, called cells, and that a spectral wave model estimates the average value of the unknowns in each cell. The definition of cell depends on the numerical scheme. In regular grids, the cells are all the rectangles that form when the domain is subdivided with a regular lattice. In triangular meshes, the nodes are the reference points of the median dual cells. In SMC meshes, cells are rectangular, as in regular grids, and their size and position depend on the resolution of the local lattice.

Given a cell (let us call it A, Fig. 1 ab) UOST estimates, for each spectral component, the effect of a) the unresolved features located in A (Local Dissipation, LD); b) the unresolved features located upstream of A, and projecting their shadow on A (Shadow Effect, SE). For the estimation of SE, an upstream polygon A' is defined for each cell/spectral component, as the intersection between the joint cells neighboring A (cells B, C and D in Fig. 1 a,b), and the flux upstream of A.

For each cell or upstream polygon, and for each spectral component, two different transparency coefficients are estimated. 1) The overall transparency coefficient α: a value of 1 for this coefficient indicates a cell (or upstream polygon) completely free of unresolved obstacles, while $\alpha = 0$ indicates a totally obstructed cell/upstream polygon. 2) A layout-dependent transparency β, defined as the average transparency of cell sections starting from the cell upstream side. Values close to 1 represent a polygon free of obstacles, or with obstacles all located close to the downstream side. Values close to 0 indicate that the polygon is totally obstructed, and the obstacles are all located close to the upstream side of the polygon. The values of α and β are such that always $\beta \geq \alpha$. The LD and SE components of the source term can be written as (Mentaschi et al., 2015b)

$$\left.\frac{\partial F}{\partial t}\right|_{LD}(\mathbf{x},\mathbf{k}) = -\frac{1-\beta_l}{\beta_l}\frac{c_g}{\Delta L}F \tag{1}$$

$$\left.\frac{\partial F}{\partial t}\right|_{SE}(\mathbf{x},\mathbf{k}) = -\left(\frac{\beta_u}{\alpha_u}-1\right)\frac{c_g}{\Delta L}F\ , \tag{2}$$

where F is the spectral density, $\mathbf{x}$ is the position of the cell in space, $\mathbf{k}$ is the wave vector of the spectral component, c_g is the group velocity, ΔL is the path length of the spectral component in the cell. The subscripts l and u of α and β indicate that these coefficients can be referred, respectively, to the cell and to the upstream polygon. We need to mention, that theoretically a formulation based on source terms, such as UOST, is unable to model total blocking. However, we notice that the LD and SE contributions diverge in case of total blocking, virtually providing infinite dissipation. In practice a high limit is imposed to the maximum allowed dissipation, able to dump almost completely the energy. For a more detailed discussion of **1** and **2** the reader is referred to Mentaschi et al. (2015b).

The estimation of the transparency coefficients from a real bathymetry is a major challenge in the parameterization of unresolved obstacles, and the reason for the development of automation software such as Gridgen (Chawla and Tolman, 2008). The package alphaBetaLab comes as a logical generalization of Gridgen, and automates the estimation of the upstream polygon and of the coefficients α_l, β_l, α_u, β_u, without making any assumption on the geometrical nature of the cells, other than considering them as free polygons. This involves, that it can be applied to any type of mesh, including unstructured finite elements and SMC meshes. We need to mention that while UOST would be able to modulate the energy dissipation with the spectral frequency, only the direction is currently considered in alphaBetaLab. Given a polygon alphaBetaLab estimates the transparency coefficient α as a function of the cross section σ of the unresolved obstacles for each directional bin (Fig. 1 c,d):

$$\alpha(\mathbf{x},\mathbf{k}) = 1 - \sigma(\mathbf{x},\mathbf{k})\ . \tag{3}$$

The coefficient β is estimated slicing the cell into N_s subsections starting from the upstream side, along the direction of each propagating spectral component (i.e. the sides of the slices are normal to the propagation direction), the last slice being equal to the whole polygon. In the case shown in **1** c, where the algorithm is illustrated for $N_s = 4$ and for a spectral component propagating along the x axis for a rectangular cell, the first slice would span from x_0 to x_1, the last from x_0 to x_4. The coefficient β is then estimated as the average α of all the slices. In the present study $N_s = 8$ slices have been considered for each directional bin. For more details about the definition and the estimation of β, the reader is referred to Mentaschi et al. (2015b). For cells intersecting large land bodies for more than 10% of their surface, α and β are set to 1 (no unresolved obstacles), because there UOST would conflict with the resolved part of wave sheltering and shallow water dynamics.

We need to underline, that both UOST and Gridgen do not provide full subscale modelling, but only a parameterization of the energy dissipation due to unresolved obstacles. Full subscale modelling would require also a parameterization of refraction, reflection, as well as shallow water dynamics (Mentaschi et al., 2015b).

2.1. Time resolution

In spectral models adopting the fractional steps method (Yanenko, 1971), setting a source-term time step (i.e. the time step of application of the source terms) much larger than the critical Courant-Friedrichs-Lewy (CFL) time step (i.e. the time required for the fastest spectral component to cross a specific cell) can lead to inaccuracies, especially if the wave climate and wind forcing change significantly in the length scale of one cell (Tolman, 2014, Appendix B1); this can happen, for example, in extreme conditions. In the case of subscale

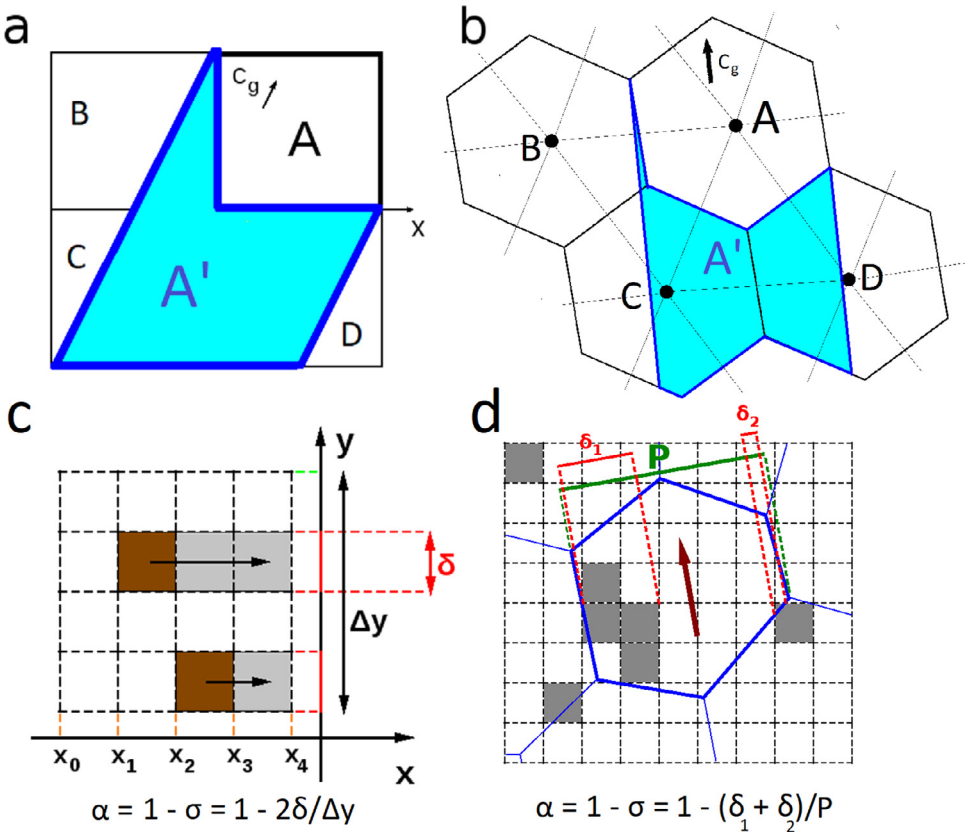

Fig. 1. a: A square cell (A) and its upstream polygon (A′, delimited by blue line, in light blue color) for a spectral component propagating with group velocity c_g. The joint BCD polygon represents the neighborhood polygon. b: same as a, but for a triangular mesh (the hexagons approximate the median dual cells). c: Computation of α and β for a square cell, $N_s = 4$, and a spectral component propagating along the x axis. The brown squares represent unresolved obstacles, the grey squares are sheltered by the unresolved obstacles. The total cross section of the unresolved obstacles in this case is 2δ, therefore we have α = 0.5. β is computed as the average α of the sections between x_0-x_1, x_0-x_2, x_0-x_3, x_0-x_4. For this example, we can easily find β = 0.6875. d: Like c, but for a hexagonal cell and for a tilted spectral component. In panel d he gray squares represent unresolved obstacles. (For interpretation of the references to color in this figure legend, the reader is referred to the web version of this article.)

modeling, significant changes in the amount of advected wave energy take place inside single cells, due to the presence of local or upstream unresolved features. Using time steps larger than the critical CFL time step for spatial propagation would results in a leakage of energy that would pass through the cell without being attenuated by UOST.

This restriction on the time step comes as a limitation of UOST with respect to Gridgen. Although in the simulations carried out in the current study the computational costs of UOST and of Gridgen are roughly equal, the adoption of a time step equal to the critical CFL time step can result in computationally more expensive models, depending on the specific application. There are, however, practices and possible future developments that can alleviate this limitation.

(1) Using unstructured grids, especially with implicit schemes, a modeler may choose the minimum size of a cell where a complete parameterization of unresolved obstacles is required, and set consequently the source-term time step of the model to the resulting critical CFL time step. In other words, only cells large enough, for their critical CFL time steps to be larger than the source-term time step would be considered in UOST. This would be enough to model correctly, for example, conditions when high-resolution-resolved coasts are sheltered by low-resolution-resolved coral reefs/cliffs/tiny islands.
(2) In models adopting the fractional steps method, the application of the UOST source term could be done for each spectral component according to the propagation time step, rather than to the source-term time step. This strategy would remove the limitation for explicit schemes, but not for implicit schemes, where the propagation time step can exceed the critical CFL time step.
(3) Let us define CFL critical length L_{CFL} as the distance covered by a spectral component in a single time step. A future development of alphaBetaLab may distribute the effect of the unresolved obstacles of a cell smaller than L_{CFL} through several contiguous cells, in order to cover a distance L_{CFL}. Such an implementation would remove the limitation also for implicit numerical schemes with a time step above the critical CFL one. Besides, implicit schemes with a time step larger than the critical CFL one, are known for providing good spatial means of the variables, but the numerical accuracy at single cells is limited (e.g. Choi and Moin, 1994).

3. Model setup and runs

The UOST approach was implemented in the third generation spectral wave model WAVEWATCH III (hereinater WW3, Tolman, 2014), version 4.18.

For all the different spatial resolutions, the spectral resolution consists of 25 frequencies exponentially spaced ranging from 0.04 Hz corresponding to a period of 25 s to 0.45 Hz (about 2 s), and 24 directions. The source term ST4 (Ardhuin et al., 2010b) was employed to represent the growth/dissipation of the waves. The source-term time step, i.e. the time step of application of the source terms (that in WW3 coincides with the main time step) was set to 1800 s for all the simulations. The models ran on a global domain, but subscale modelling was applied and investigated only in the area of the Caribbean (−100°E < longitude < −55°E, 5°N < latitude < 30°N). The forcing consists of CFSR winds, and the time horizon is 10 years, ranging from 2000 to 2009.

The simulations were performed at different resolutions employing different approaches for subscale modelling. UOST was applied to a regular mesh with a resolution of 1.5 deg (simulation UOST15). The same grid was used with the propagation-scheme-based approach implemented in WW3 (hereinafter Gridgen, Chawla and Tolman, 2008, simulation GRIDGEN15), and with no subscale modelling (simulation NOSM15). To compare the skills of the 1.5 deg simulations with higher resolution ones, a subsequent run was carried out with a resolution of 0.4 deg (simulation GRIDGEN04). These simulations are summarized in Table 1. For the Gridgen runs, the obstruction coefficients have been estimated using the software package distributed with the source code

Table 1
Carried out simulations, their resolution, subscale modelling approach and simulation skills in terms of Normalized Root Mean Square Error (NRMSE), Normalized Bias (NBI) and Normalized Bias of the yearly maxima (NBI_{ymax}).

Simulation	Resolution	Subs. model.	NRMSE	NBI	NBI_{ymax}
NOSM15	1.5°	None	27.97%	19.07%	9.00%
UOST15	1.5°	UOST	17.13%	−0.54%	−3.73%
GRIDGEN15	1.5°	Gridgen	17.87%	−1.17%	−2.69%
GRIDGEN04	0.4°	Gridgen	17.80%	−1.38%	−3.64%

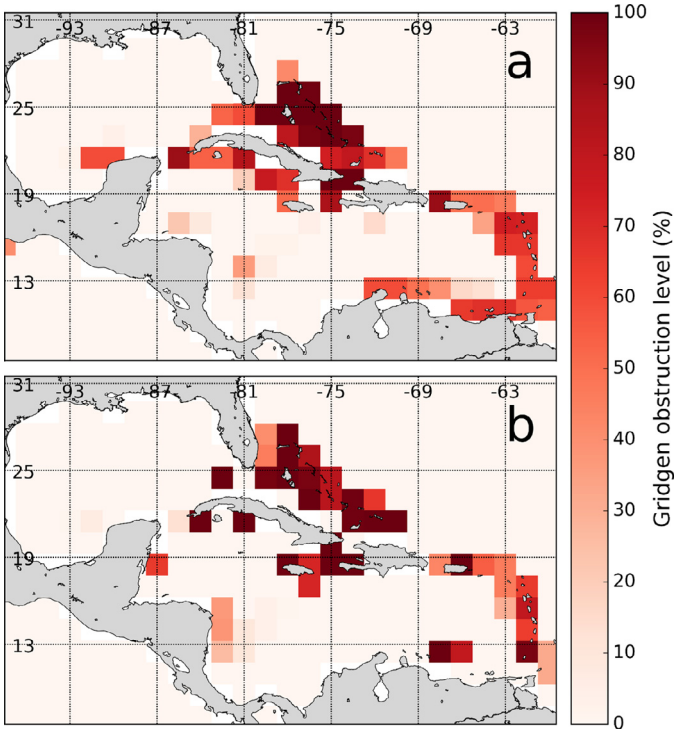

Fig. 2. Obstruction coefficients estimated for the Gridgen simulation, for longitudinal (a) and latitudinal (b) propagation. In cells with values close to 0 there is no dissipation. Values close to 1 indicate total blocking.

of WW3 (Fig. 2).

For the computation of the transparency coefficients needed by UOST, alphaBetaLab was employed. The resulting values of $\alpha_l(\theta)$ and $\beta_l(\theta)$ (i.e. the local transparency coefficients of the cell) are shown in Fig. 3a for each cell as a pie diagram, while $\alpha_u(\theta)$, $\beta_u(\theta)$ (i.e. the transparency coefficients of the upstream polygon) are shown in Fig.3b. We need to mention, that α and β can be represented in the same pie diagram, because, always, $\beta \geq \alpha$. Therefore, when the blue value is not visible, we are in a situation when $\beta = \alpha$. For those cells with α and β uniformly equal to 1, i.e., cells without unresolved obstacles, a full pie would be plotted, but in such cases the pie is not plotted.

For the validation, the simulated significant wave height (H_s) was compared with measurements of satellite altimeters (Queffeulou and Croizé-Fillon, 2014). Since the spatial/temporal resolution of satellite data along the satellite tracks is much higher than that of the model, satellite data have been binned over latitudinal spans of 1.5° (coincident with the latitudinal limits of the coarser grid cells) and averaged, before comparing them with model data. The average skills of the models are quantified estimating, for each of the cells, the Normalized Root Mean Square Error (NRMSE), the Normalized Bias (NBI), and the Normalized Bias of the mean annual maxima (NBI_{ymax}) (Mentaschi et al., 2013). The overall value of these indicators is computed by averaging them over the cells covering the Caribbean Sea region. The directional spectra of the different model set-ups were compared at location A (Fig. 4) during the tropical storm Helen in September 2000. Further, at location B (Fig. 4), where the buoy 42,059 of the US National Data Buoy Center (NDBC) is moored, H_s, the mean period T_{-10} (Holthuijsen, 2007; Komen et al., 1994) and the frequency spectra of the different model set-ups were compared with the ones measured by the buoy.

4. Model skill in the Caribbean sea

The skills of UOST15 and GRIDGEN15 for the examined case are qualitatively similar, and both can be considered as a major improvement compared with NOSM15 (Table 1). In the Caribbean Sea, the model without subscale modelling has a strong positive bias of about 20% of mean H_s, while GRIDGEN15 and UOST15 have a weak negative bias of about −1% and −0.5%, respectively. The performance measured with NRMSE of H_s shows a similar trend, NOSM15 having a high NRMSE, close to 30% and the other simulations with a much lower value, between 17% and 18%. UOST15 is the overall best performing with NRMSE = 17.13%. The positive bias of annual maxima is 9% for NOSM15 while it ranges between −2.7% and −3.7% for the other simulations. In this case UOST15 performs slightly worse compared to GRIDGEN15 (about −3.7% vs −2.7%), but its skills are similar to GRIDGEN04 (about −3.6%). Interestingly, increasing the spatial resolution to 0.4 deg in GRIDGEN04 does not have a significant impact on the overall skills of the model in this domain, neither in terms of average H_s nor in terms of yearly maxima. This can be explained with the fact that UOST and Gridgen parameterize the large-scale effect of small bathymetric features reasonably well, and consequently, the average skills of low and high-resolution models on large areas are comparable. The benefit of high resolution would be better appreciated considering the model performance in proximity of the coast, or of small features not resolved in low resolution models, or in the development of mesoscale-dominated extreme events, such as tropical cyclones (provided these events are adequately modeled in the wind forcing). This consideration underlines the importance in wave modelling of subscale parameterizations such as UOST and Gridgen.

Cell-by-cell skills of UOST15 and GRIDGEN15 are illustrated in Fig. 4. UOST15 performs generally better in the area around Florida, the Bahamas and Cuba. In this area, both UOST15 and GRIDGEN15 are affected by strong positive bias, but in UOST15 the bias is reduced, in some cells by more than 30%. The explanation is that the Bahamas islands have an elongated shape lying in direction NW-SE, normal to the dominant wave climate with energy coming mainly from NE. In the UOST scheme the transparency coefficients α and β are modulated with the direction. This can be seen clearly in Fig. 3 a,b, where at the Bahamas islands the α-β pies are clearly tilted in NW-SE direction, involving a stronger dissipation for spectral components coming from NE than for those coming from NW. Instead, in Gridgen only two transparencies are considered, one in longitudinal and the other in latitudinal direction (Fig. 2). Consequently, the dissipation in direction NE-SW is underestimated. The directionality of unresolved obstacles plays a role also West of the Lesser Antilles, which have a geometry clearly tilted around the Eastern Caribbean (Fig. 3a,b). The skill of UOST15 is considerably worse than GRIDGEN15 South of Cuba, exhibiting a strong underestimation of H_s. This is due to the inability of the alphaBetaLab algorithm to determine which parts of Cuba should be considered as unresolved. The cells close to large land bodies are generally modelled correctly without subscale modelling and that is why both alphaBetaLab and Gridgen, do not compute a transparency coefficient for cells close to continental coasts. In this case, Cuba provides a limiting case, because at a resolution of 1.5° parts of it are correctly represented as land, while other parts need to be parameterized with subscale modelling. Gridgen is better than alphaBetaLab in detecting in which cases subscale modelling is needed. The current implementation of alphaBetaLab estimates transparency coefficients in too many cells, and the dissipation South of Cuba is consequently overestimated.

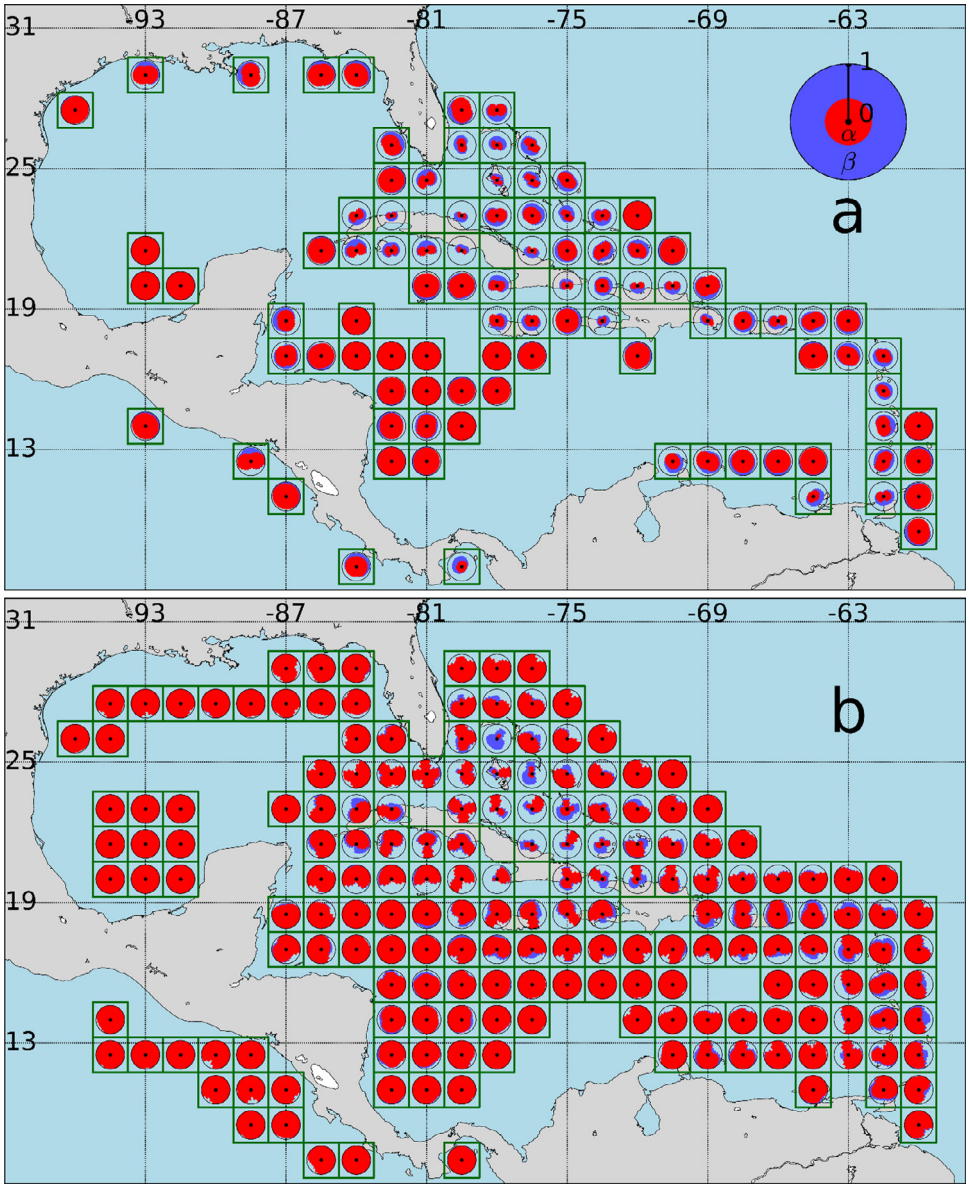

Fig. 3. Coefficients α and β for the local effect (a) and for the shadow (b), represented for each cell as a function of the angle of propagation of the spectral component. Values of α and β close to 0 indicate total dissipation. Values of α and β close to 1 indicate no dissipation. $\alpha \leq \beta$ always, therefore, if the sole red pie is visible, then $\beta \approx \alpha$. (For interpretation of the references to color in this figure legend, the reader is referred to the web version of this article.)

Indeed, alphaBetaLab estimates low transparency coefficients α and β in cells intersecting the coasts of Cuba (Fig. 3), whereas Gridgen correctly identifies them as coastal cells, with transparency equal to 1 (obstruction level equal to 0, Fig. 2).

The directional spectra were examined and compared at location A, South of the Virgin Island (coordinates −64.81°E, 16.775°N, Fig. 4) during the tropical storm Helen in September 2000 (Fig. 5). Location A was chosen because it is placed along the storm track of a medium size tropical storm like Helen, downstream of the Lesser Antilles. At this location both UOST15 and GRIDGEN15 perform generally well, but GRIDGEN15 slightly underestimates H_s. For this tropical storm the time series of H_s for UOST15, GRIDGEN15 and GRIDGEN04 lie fairly close together, far below the strongly overestimating NOSM15 (Fig. 5a). We notice that H_s estimated by GRIDGEN04 lies between GRIDGEN15 and UOST15. The spectra of September 18, 2000 simulated by UOST15, GRIDGEN15 and GRIDGEN04 for location A, have a similar shape, with an intense peak directed towards SW, corresponding to the moving direction of the tropical storm, and a weaker peak directed towards NW (Fig. 5b,c,e). In UOST15 the SW peak is more intense than in the other models, due to weaker dissipation associated with the small islands NE of location A. The NW peak is alike in all three simulations. in this case, spectra and H_s of GRIDGEN15 and GRIDGEN04 are more similar than that of UOST15. This could depend from the fact location A is in proximity of small islands, that even in GRIDGEN04 require the Gridgen approach for a correct parameterization.

A further test was performed at location B, South-West of Puerto Rico (coordinates −67.51°E, 15.252°N, Fig. 4), in January 2008. Here frequency spectra and bulk parameters modeled by the different simulations were compared with the 12 h moving average of the ones measured at buoy 42,059 of NDBC (Fig. 6). At this location both UOST15 and GRIDGEN15 generally underestimate H_s (Fig. 4d,e), likely due to a tendency of parameterization TEST451f of Ardhuin et al. (2010a) to underestimate short fetches with CFSR wind data (Kazeminezhad and Siadatmousavi, 2017; Mentaschi et al., 2015a). However, neglecting the unresolved obstacles leads to strong overestimation of both H_s and T_{-10} (Fig. 6a,b). The values simulated by UOST and GRIDGEN04, both for bulk parameters and frequency spectra, are remarkably similar. The differences between the buoy

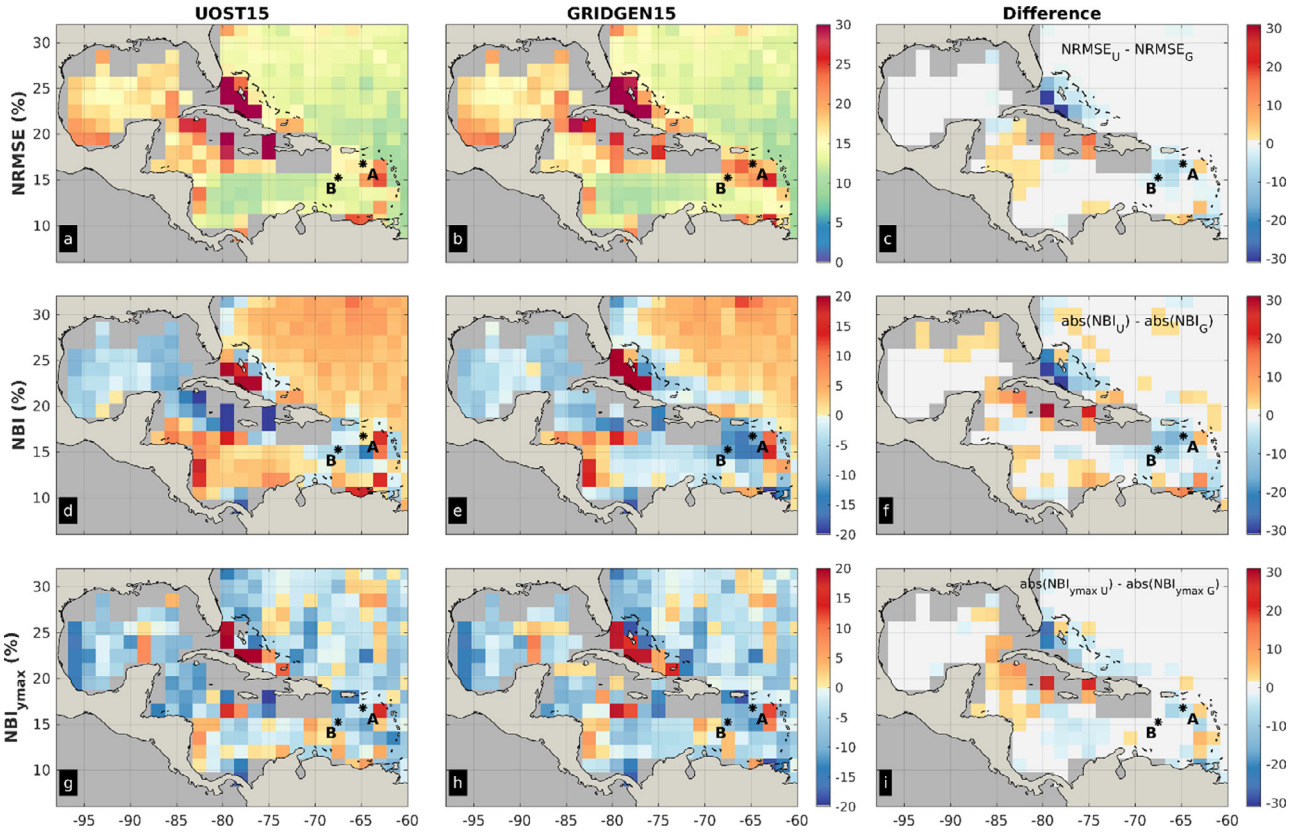

Fig. 4. Normalized Root Mean Squared Error (NRMSE), Normalized Bias (NBI), and Normalized Bias of the yearly maxima (NBI_{ymax}) for UOST15 (a, d, g) and GRIDGEN15 (b, e, h), for each cell of the 1.5 deg domain, and cell-by-cell comparison (c, f, i). Point A in panels c, f, i represents the location where tropical storm Helen has been investigated.

spectra and the ones modeled by UOST-GRIDGEN are party due to the underestimation of the model, partly to limitations of the Discrete Interaction Approximation (DIA), that tends to overestimate the energy transfer from the peak to higher and lower frequencies (Hasselmann et al., 1985; Rogers and Van Vledder, 2013). Furthermore, the broader shape of the modeled spectra, compared with the measured ones, may be related with the underestimation of both wave growth (that takes place mainly at high frequencies) and wave dissipation at low

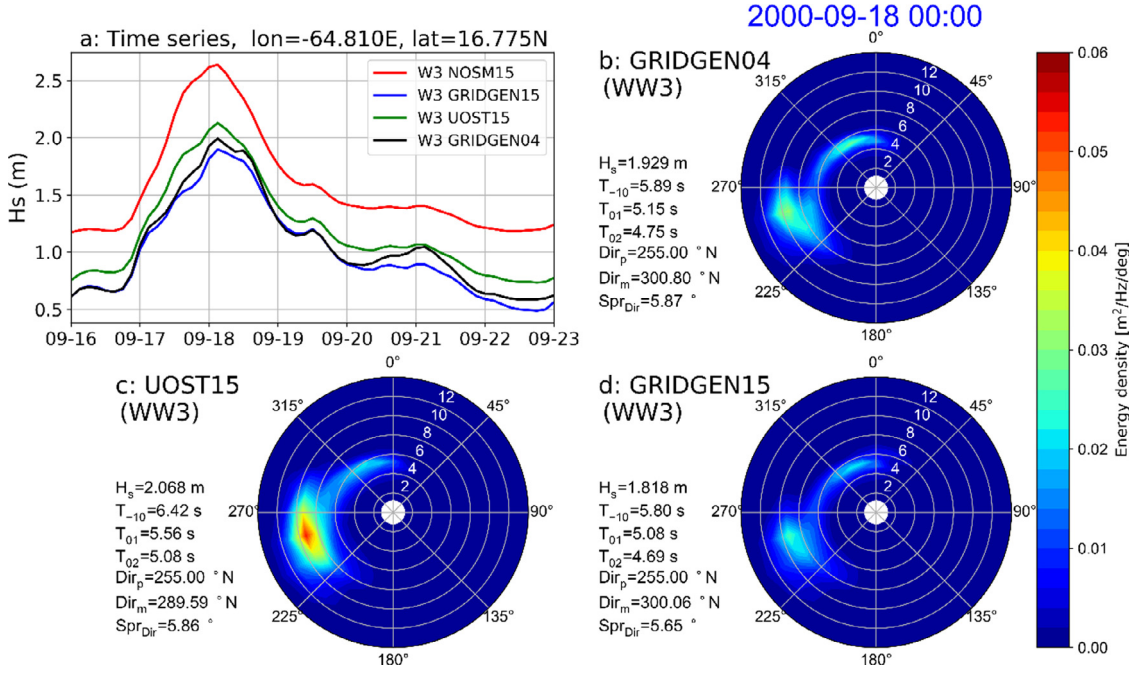

Fig. 5. Tropical Storm Helen: time series of significant wave height for each simulation (a) and spectra for September 18 2000, as modelled by GRIDGEN04 (b), UOST15 (c) GRIDGEN15 (d). In panels b, c, d the bulk parameters are listed, together with the spectrum rose diagrams.

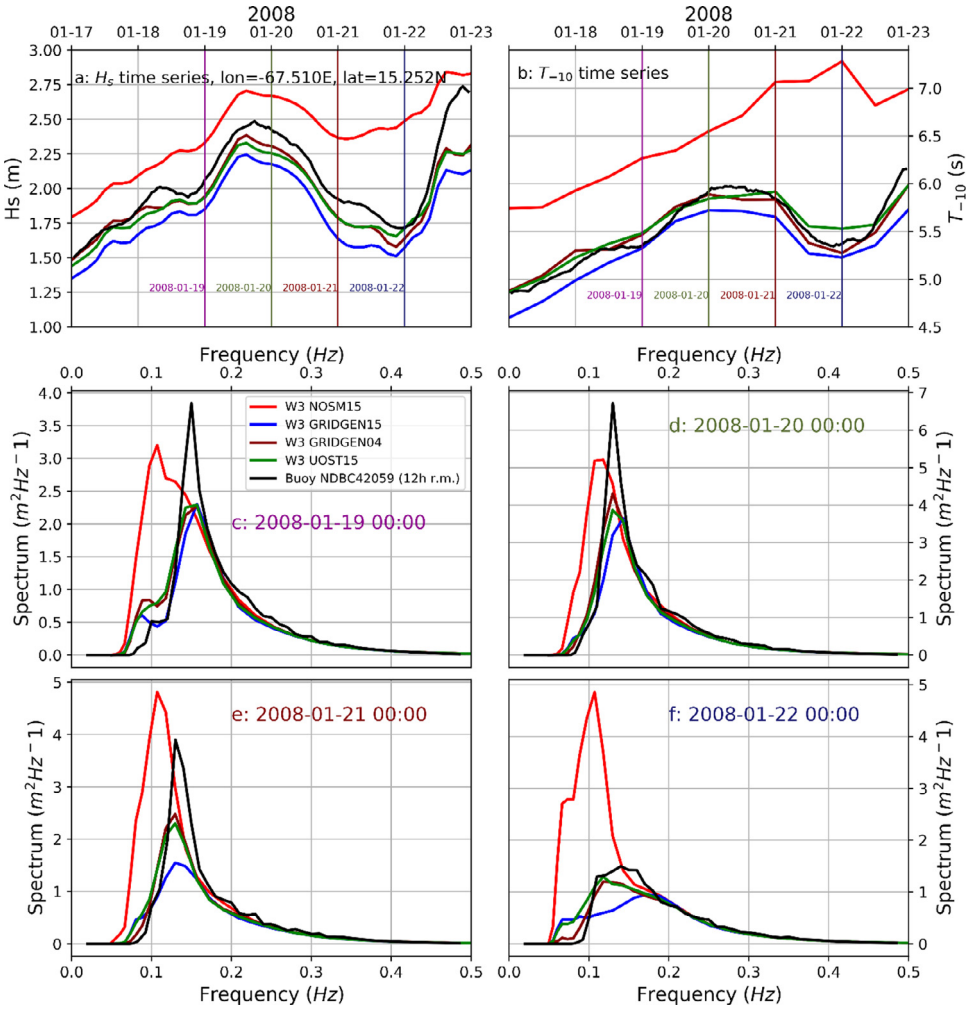

Fig. 6. Comparison models-buoy measurements at buoy 42,059 of the National Data Buoy Center (NDBC), for an event in January 2008. Time series of Hs (a), and mean period T_{-10} (b). Frequency spectra at different time stamps (cdef). The timing of the spectra is indicated in ab with vertical lines. The buoy data have been processed with a 12 h running mean.

frequencies. In the comparison of the frequency spectra, NOSM is found overestimating mainly at low frequencies corresponding to swell, that in UOST and GRIDGEN15 are better modelled thanks to the parameterization of unresolved obstacles.

5. Final remarks

Our analysis indicates that UOST can be successfully applied to real-world applications. In general, UOST performances are comparable to the ones of the established approach for subscale modelling. In some locations, where a correct parameterization of the unresolved obstacles is crucial, like downstream of the Bahamas and the Antilles islands, the skills of UOST benefit of its taking into account the directional layout of the unresolved obstacles. In other areas UOST underperforms, and this can be attributed to limits of the current implementation of alphaBetaLab, rather than to the UOST approach itself, for example South of Cuba, where strong dissipation is modelled in areas with coastal features that should not be considered unresolved (Fig. 3). However, the real advantage of UOST is its applicability to any numerical scheme, and the development of alphaBetaLab is a significant step towards this generalization: the only further step necessary to implement UOST on a particular mesh is to provide alphaBetaLab the mesh definition as a set of polygonal cells. For example, an implementation for triangular grids, based on an approximate estimation of the median dual cell, is already available, although it requires further test.

A problem of the current implementation of alphaBetaLab is that it is rather slow. It takes about 2 minutes to estimate the transparency coefficients in the small domain considered in this study, even parallelizing the computation on 12 highly performing Xeon® cores, while runs on bigger domains would require much longer times. While this is surely a secondary aspect (alphaBetaLab has to run once for one domain), a better optimized version of the algorithm would be useful for faster development and testing.

The source code of alphaBetaLab is freely available at https://github.com/menta78/alphaBetaLab. For the sake of reproducibility, the related methods article (Mentaschi et al., 2018) contains detailed instructions to replicate the case study on the Caribbean Sea, and a description of the architecture of alphaBetaLab.

Acknowledgment

The research leading to these results has received funding from the JRC of the European Commission as part of the COAST and ADAPTATION projects. We thank the anonymous reviewers, for helping with their comments to substantially improve the quality of this manuscript.

Supplementary materials

Supplementary material associated with this article can be found, in the online version, at doi:10.1016/j.ocemod.2018.04.003.

References

Ardhuin, F., Rogers, E., Babanin, A.V., Filipot, J.-F., Magne, R., Roland, A., van der Westhuysen, A., Queffeulou, P., Lefevre, J.-M., Aouf, L., Collard, F., Ardhuin, F., Rogers, E., Babanin, A.V., Filipot, J.-F., Magne, R., Roland, A., Westhuysen, A., van der, Queffeulou, P., Lefevre, J.-M., Aouf, L., Collard, F., 2010a. Semiempirical dissipation source functions for ocean waves. part I: definition, calibration, and validation. J. Phys. Oceanogr. 40, 1917–1941. http://dx.doi.org/10.1175/2010JPO4324.1.

Ardhuin, F., Rogers, E., Babanin, A.V, Filipot, J.-F., Magne, R., Roland, A., van der Westhuysen, A., Queffeulou, P., Lefevre, J.-M., Aouf, L., Collard, F., 2010b. Semiempirical dissipation source functions for ocean waves. Part I: definition, calibration, and validation. J. Phys. Oceanogr. 40, 1917–1941.

Booij, N., Ris, R.C., H., H.L., 1999. A third generation wave model for coastal regions, Part I, model description and validation. J. Geophys. Res. 7, 649–666.

Chawla, A., Tolman, H.L., 2008. Obstruction grids for spectral wave models. Ocean Model 22, 12–25. http://dx.doi.org/10.1016/j.ocemod.2008.01.003.

Choi, H., Moin, P., 1994. Effects of the computational time step on numerical solutions of turbulent flow. J. Comput. Phys. 113, 1–4. http://dx.doi.org/10.1006/jcph.1994.1112.

Hardy, T.A., Mason, B.L., McConochie, J.D., 2000. A wave model for the great barrier reef. Ocean Eng 28, 45–70.

Hasselmann, S., Hasselmann, K., Allender, J.H., Barnett, T.P., Hasselmann, S., Hasselmann, K., Allender, J.H., Barnett, T.P., 1985. Computations and parameterizations of the nonlinear energy transfer in a gravity-wave specturm. Part II: parameterizations of the nonlinear energy transfer for application in wave models. J. Phys. Oceanogr. 15, 1378–1391. doi:10.1175/1520-0485(1985)015<1378:CAPOTN>2.0.CO;2.

Holthuijsen, L.H., 2007. Waves in oceanic and coastal waters, waves in oceanic and coastal waters. doi:10.1017/CBO9780511618536.

Kazeminezhad, M.H., Siadatmousavi, S.M., 2017. Performance evaluation of WAVEWATCH III model in the Persian Gulf using different wind resources. Ocean Dyn 67, 839–855. http://dx.doi.org/10.1007/s10236-017-1063-2.

Komen, G.J., Cavaleri, L., Donelan, M., Hasselmann, K., Hasselmann, S., Janssen, P.A.E.M., 1994. Dynamics and Modelling of Ocean Waves. Cambridge University Press, Cambridge. http://dx.doi.org/10.1017/CBO9780511628955.

Li, J.-G., 2011. Global transport on a spherical multiple-cell grid. Mon. Weather Rev. 139, 1536–1555. http://dx.doi.org/10.1175/2010MWR3196.1.

Mentaschi, L., Besio, G., Cassola, F., Mazzino, A., 2015a. Performance evaluation of wavewatch III in the mediterranean sea. Ocean Model 90, 82–94. http://dx.doi.org/10.1016/j.ocemod.2015.04.003.

Mentaschi, L., Besio, G., Cassola, F., Mazzino, a., 2013. Problems in RMSE-based wave model validations. Ocean Model 72, 53–58. http://dx.doi.org/10.1016/j.ocemod.2013.08.003.

Mentaschi, L., Kakoulaki, G., Vousdoukas, M., Voukouvalas, E., Feyen, L., Besio, G., 2018. UOST, alphaBetaLab and wavewatch: running a case study in the Caribbean. MethodsX.

Mentaschi, L., Pérez, J., Besio, G., Mendez, F.J., Menendez, M., 2015b. Parameterization of unresolved obstacles in wave modelling: a source term approach. Ocean Model 96, 93–102. http://dx.doi.org/10.1016/j.ocemod.2015.05.004.

Queffeulou, P., Croizé-Fillon, D., 2014. Global altimeter SWH data set.

Rogers, W.E., Van Vledder, G.P., 2013. Frequency width in predictions of windsea spectra and the role of the nonlinear solver. Ocean Model 70, 52–61. http://dx.doi.org/10.1016/j.ocemod.2012.11.010.

Roland, A., 2008. Development of WWM II: Spectral Wave Modelling on Unstructured Meshes. Technische Universitat Darmstadt, Institute of Hydraulic and Water Resources Engineering.

Tolman, H.L., 2014. User manual and system documentation of WAVEWATCH III version 4.18.

Tolman, H.L., 2003. Treatment of unresolved islands and ice in wind wave models. Ocean Model 5, 219–231.

Tuomi, L., Pettersson, H., Fortelius, C., Tikka, K., Bjorkqvist, J., Kahma, K.K., 2014. Wave modelling in archipelagos. Coast. Eng. 83, 205–220.

Yanenko, N.N., 1971. The Method of Fractional Steps. Springer, Berlin Heidelberg, Berlin, Heidelberg. http://dx.doi.org/10.1007/978-3-642-65108-3.

Zijlema, M., 2010. Computation of wind-wave spectra in coastal waters with SWAN on unstructured grids. Coast. Eng. 57, 267–277. http://dx.doi.org/10.1016/j.coastaleng.2009.10.011.